Pitfalls and Common Findings in ^{68}Ga-FAPI PET: A Pictorial Analysis

Lukas Kessler[1,2], Justin Ferdinandus[1,2], Nader Hirmas[1,2], Fadi Zarrad[1,2], Michael Nader[1,2], David Kersting[1,2], Manuel Weber[1,2], Sandra Kazek[1,2], Miriam Sraieb[1,2], Rainer Hamacher[2,3], Katharina Lueckerath[1,2], Lale Umutlu[2,4], Wolfgang P. Fendler[1,2], and Christoph Rischpler[1,2]

[1]*Department of Nuclear Medicine, University Hospital Essen, University of Duisburg–Essen, Essen, Germany;* [2]*German Cancer Consortium, University Hospital Essen, University of Duisburg–Essen, Essen, Germany;* [3]*Department of Medical Oncology, West German Cancer Center, University Hospital Essen, University of Duisburg–Essen, Essen, Germany; and* [4]*Institute of Diagnostic and Interventional Radiology, University Hospital Essen, University of Duisburg–Essen, Essen, Germany*

Fibroblast activation protein inhibitor (FAPI) PET/CT is a new tool in the diagnostic workup of cancer. With a growing volume of applications, pitfalls and common findings need to be considered for ^{68}Ga-FAPI PET/CT image interpretation. The aim of this study was to summarize common findings and report pitfalls in ^{68}Ga-FAPI PET/CT. **Methods:** Ninety-one patients underwent whole-body PET/CT with either FAPI-04 ($n = 25$) or FAPI-46 ($n = 66$). Findings were rated in a consensus session of 2 experienced readers. Pitfalls and common findings were defined as focal or localized uptake above the background level and categorized as unspecific or nonmalignant and grouped into degenerative, muscular, scarring/wound-healing, uterine, mammary gland, and head-and-neck findings. The frequency of findings was reported on a per-patient and per-group basis, and SUV_{max}, SUV_{mean}, and SUV_{peak} were measured. **Results:** Non–tumor-specific uptake was found in 81.3% of patients. The most frequent finding was uptake in degenerative lesions (51.6%), with a mean SUV_{max} of 7.7 ± 2.9, and head-and-neck findings (45.1%). Except for the salivary glands, the uptake values did not differ between 10 and 60 min after injection in most findings. Uterine uptake was found in most women (66.7%), with a mean SUV_{max} of 12.2 ± 7.3, and uptake correlated negatively with age (SUV_{max}, $r = -0.6$, $P < 0.01$; SUV_{peak}, $r = -0.57$, $P < 0.01$; SUV_{mean}, $r = -0.58$, $P < 0.01$). **Conclusion:** Pitfalls include non–tumor-specific ^{68}Ga-FAPI uptake in degenerative lesions, muscle, the head and neck, scarring, the mammary glands, or the uterus. Here, we summarize the findings to help readers avoid common mistakes at centers introducing ^{68}Ga-FAPI PET/CT.

Key Words: cancer imaging; FAPI; fibroblast activation protein; PET; pitfalls

J Nucl Med 2022; 63:890–896
DOI: 10.2967/jnumed.121.262808

Fibroblast-activation protein (FAP) is a protein commonly expressed in cancer-associated fibroblasts, which are present in the stroma of 80%–90% of all cancers. Mediators produced by carcinoma-associated fibroblasts influence tumor cells on many levels by promoting tumor angiogenesis, migration, and proliferation (*1,2*). In normal fibroblasts, the structurally similar enzyme dipeptidyl peptidase 4 is expressed, whereas FAP is not expressed (*3,4*). On this basis, a metaanalysis of 15 studies proved that FAP overexpression in solid tumors is associated with a poor outcome and is distinctly present in tumor cells compared with normal tissue (*5*). Therefore, FAP has become a highly promising target for novel cancer therapeutics and diagnostics.

In 2018, Loktev et al. showed that DOTA-containing FAP inhibitors (FAPIs) can be coupled with ^{68}Ga and used for PET imaging of multiple tumor entities, such as breast, colon, lung, and pancreatic cancer (*6*). Since then, clinical evidence has been growing for FAP-targeted PET.

TABLE 1
Patient Characteristics

Characteristic	Data
Overall	91
Age (y)	
Mean	57.4 (SD, 13.3)
Median	58.0 (range, 18.0–83.0)
Sex	
Female	42 (46.2%)
Male	49 (53.8%)
Oncologic diagnosis	76
Pancreatic cancer	28 (36.8%)
Sarcoma	16 (21.1%)
Lung cancer	10 (13.2%)
Other	22 (28.9%)
Nononcologic diagnosis	15
CAD	10 (66.7%)
Atrial fibrillation	3 (20.0%)
Other	2 (13.3%)
FAP radiotracer	
FAPI04	25 (27.5%)
FAPI46	66 (72.5%)

CAD = coronary artery disease.
Data are number followed by percentage in parentheses, except for age.

Received Jul. 1, 2021; revision accepted Aug. 20, 2021.
For correspondence and reprints, contact Lukas Kessler (lukas.kessler@uk-essen.de).
Published online Oct. 7, 2021.

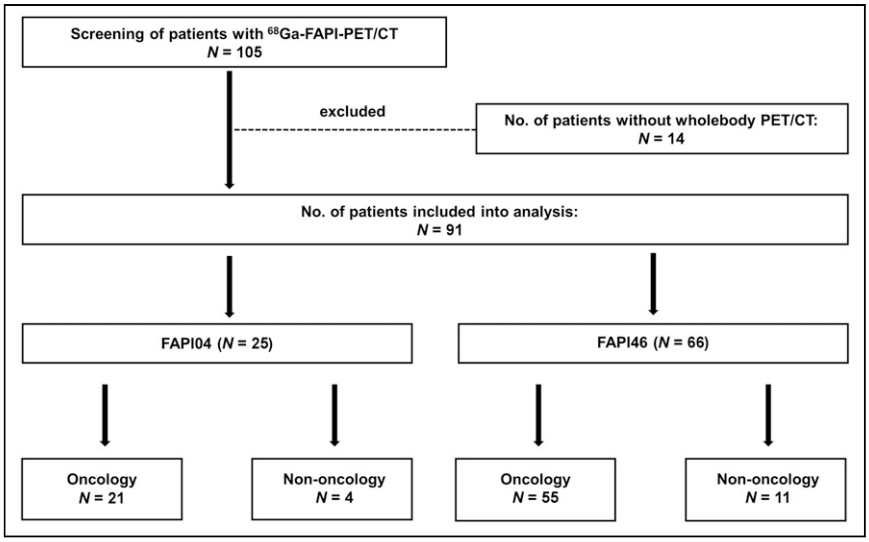

FIGURE 1. Patient selection flowchart.

It was recently shown that ^{68}Ga-FAPI PET can identify tumor lesions in various malignancies, with clinically beneficial tracer kinetics and lower tracer-to-background ratios than for ^{18}F-FDG (*7–10*). Furthermore, ^{68}Ga-FAPI showed a biodistribution similar to that of ^{18}F-FDG, with lower background uptake (*7*). Because tracer kinetics are independent from blood glucose levels, dietary arrangements are not needed for adequate imaging. Although promising data on this new radiotracer are increasing, false-positive results have been increasingly observed as well, such as in fibrotic or scar tissue (*7*). Recently, cases of nonmalignant diseases with FAPI uptake have been emerging, leading to questioning of the initially proclaimed tumor specificity (*11–17*).

After the introduction of a novel radiotracer, various potential pitfalls emerge over time and need to be summarized for the imaging community. Challenging findings have been reported in the past, such as for prostate-specific membrane antigen PET, for which a variety of false-positive findings have been found (*18,19*).

The aim of this study was to evaluate the frequency and intensity of common unspecific uptake patterns or pitfalls in ^{68}Ga-FAPI PET/CT in oncologic and nononcologic patients. We present data from our single-center retrospective study.

MATERIALS AND METHODS

Patients

One hundred five patients who underwent clinically indicated ^{68}Ga-FAPI PET/CT with either FAPI-04 or FAPI-46 between October 2018 and July 2020 were screened for eligibility. Only patients who had undergone wholebody PET/CT were included in the analysis, which led to the exclusion of 14 patients. All patients were referred for ^{68}Ga-FAPI PET/CT by treating physicians because of diagnostic challenges in oncologic and nononcologic diseases. All reported investigations were conducted in accordance with the Helsinki Declaration and with national regulations. The retrospective analysis was approved by the local Ethics Committee (permits 20-9485-BO and 20-9777-BO). Radiolabeling and administration of ^{68}Ga-FAPI-04 and ^{68}Ga-FAPI-46 complied with national and regional regulations for unproven interventions.

Image Acquisition

PET scans were obtained on a PET/CT system (Biograph mCT or Vision; Siemens). Two scans were performed approximately 10 and 60 min after injection. The injected activity of ^{68}Ga-FAPI was 149.7 ± 37.9 MBq. All PET images were iteratively reconstructed (Vision: 4 iterations, 5 subsets, 220 × 220 matrix, gaussian filtering of 5 mm; mCT: 3 iterations and 21 subsets) with time-of-flight information, using the dedicated software of the manufacturer (syngo MI.PET/CT; Siemens). Low-dose CT was acquired for attenuation correction (30 mAs, 120 keV, 512 × 512 matrix, 3-mm slice thickness) in cases of CT imaging.

Image Evaluation

Unspecific or nontumor findings were defined as findings not related to the respective disease or the purpose of the scan. Findings were rated in a consensus session by 2 experienced nuclear medicine physicians, with availability of all clinical and imaging information, and were reported along with SUV, SUV_{max}, SUV_{peak}, and SUV_{mean} 10 min and 60 min after tracer injection. Equivocal findings that could not clearly be discriminated from tumor or malignant lesions were not measured. Findings were grouped in major categories: degenerative findings, scarring and wound healing, focal or localized muscle uptake, mammary gland uptake, uterine uptake, and head-and-neck uptake (e.g., salivary glands, extraocular muscles, and dental foci).

TABLE 2
Pitfalls Listed Separately for Categories and Groups

Pitfall	All (n = 91)	FAPI-04 (n = 25)	FAPI-46 (n = 66)	P
Unspecific or non–tumor-specific findings	74 (81.3%)	17 (68.0%)	57 (86.4%)	0.06
Bone degenerative lesions	47 (51.6%)	8 (32.0%)	39 (59.1%)	0.41
Focal or localized muscle uptake	26 (28.6%)	7 (28.0%)	19 (28.8%)	0.99
Scarring or wound healing	18 (19.8%)	4 (16.0%)	14 (21.2%)	0.77
Mammary glands	7 (7.7%)	2 (8.0%)	5 (7.6%)	0.99
Uterus (n = 36)	24 (66.7%)	7 (19.4%)	17 (47.2%)	0.99
Head and neck (dental uptake, salivary glands, nasal mucosa)	41 (45.1%)	11 (44.0%)	30 (45.5%)	0.99

Data are number followed by percentage in parentheses.

TABLE 3
Radioligand Uptake in Pitfall Lesions at 60 Minutes After Injection

Pitfall lesion	SUV_{max}	SUV_{peak}	SUV_{mean}
Degenerative lesions			
Mean	7.7 (2.9)	4.3 (1.8)	4.3 (1.8)
Median	8.0 (3.1–17.3)	4.2 (2.1–11.5)	4.1 (1.1–9)
Focal or localized muscle uptake			
Mean	6.1 (2.2)	4.2 (1.4)	3.6 (1.5)
Median	5.45 (2.14–10.6)	3.8 (1.6–7.4)	3.25 (1.27–7.1)
Scarring and wound healing			
Mean	7.7 (3.3)	4.8 (1.9)	4.6 (1.9)
Median	7.6 (2.42–13.3)	5.0 (1.92–7.5)	4.7 (1.62–7.0)
Mammary glands			
Mean	4.5 (1.5)	2.6 (0.8)	2.7 (0.8)
Median	4.3 (2.3–7.25)	2.5 (1.5–3.9)	2.6 (1.2–3.8)
Uterine uptake			
Mean	12.2 (7.3)	9.6 (5.7)	7.5 (4.7)
Median	10.2 (4.2–31.2)	7.3 (3.8–24.6)	5.6 (2.2–19.3)
Salivary glands			
Mean	3.2 (0.2)	2.4 (0.2)	2.1 (0.3)
Median	3.1 (3.1–3.5)	2.4 (2.3–2.6)	2.1 (1.8–2.3)
Pancreatic uptake			
Mean	9.7 (6.0)	6.5 (4.9)	6.3 (4.0)
Median	8.8 (3.0–17.0)	5.45 (2.0–12.3)	5.75 (1.8–10.9)

Data in parentheses are SD or range.

SUV parameters were calculated by 3-dimensional volumes of interest using e.soft software (Siemens) at a 50% isocontour. The unspecific background in the blood pool (aortic vessel content), liver, and muscle was quantified with a circular 2-cm-diameter sphere.

Statistical Analysis

Statistical analyses were performed using Prism (version 9.1.0; GraphPad Software). Quantitative values were expressed as mean ± SD or as median and range when appropriate. Data were tested for a gaussian distribution using Shapiro–Wilk testing. When there was a gaussian distribution, paired Student *t* testing was used. Nonparametric data were compared using a Mann–Whitney *U* test. For bivariate correlation analyses, Spearman or Pearson correlation coefficients were calculated. For comparison of distribution, contingency testing using the Fisher exact test was used. All statistical tests were performed 2-sided, and a *P* value of less than 0.05 was considered to indicate statistical significance.

RESULTS

Patient characteristics are given in Table 1. In total, 91 patients were included in the analysis, primarily with a diagnosis of cancer (83.5%). Twenty-five patients (27.5%) were scanned with ^{68}Ga-FAPI-04, and 66 patients (82.5%) were scanned with ^{68}Ga-FAPI-46 (Fig. 1).

In most patients (81.3%), there was at least one reported finding that was rated as not related to the respective disease and

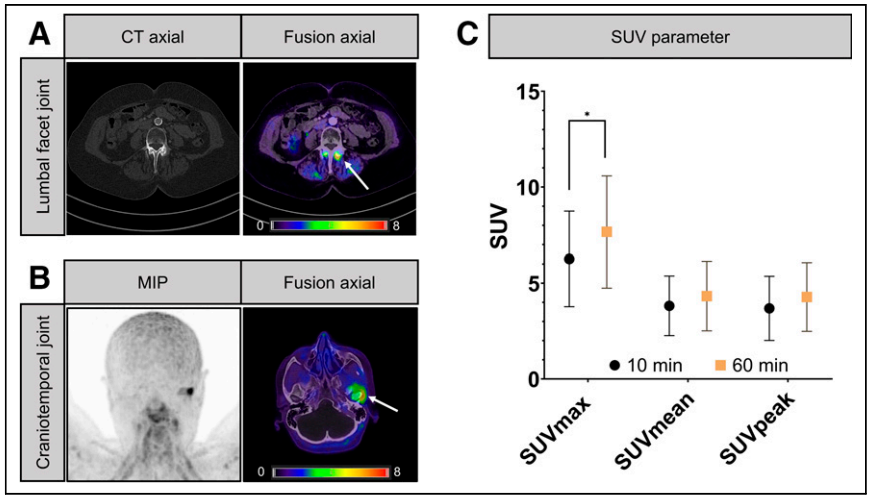

FIGURE 2. Degenerative lesions, associated mostly with joints and osteophytes. (A and B) Increased uptake of lumbar facet joints (A) and craniotemporal joint (B). (C) Uptake values showing wide range of intensity and significant increase in SUV_{max} (6.3 ± 2.5 vs. 7.7 ± 2.9, $P = 0.04$) from 10 to 60 min after injection. MIP = maximum-intensity projection.

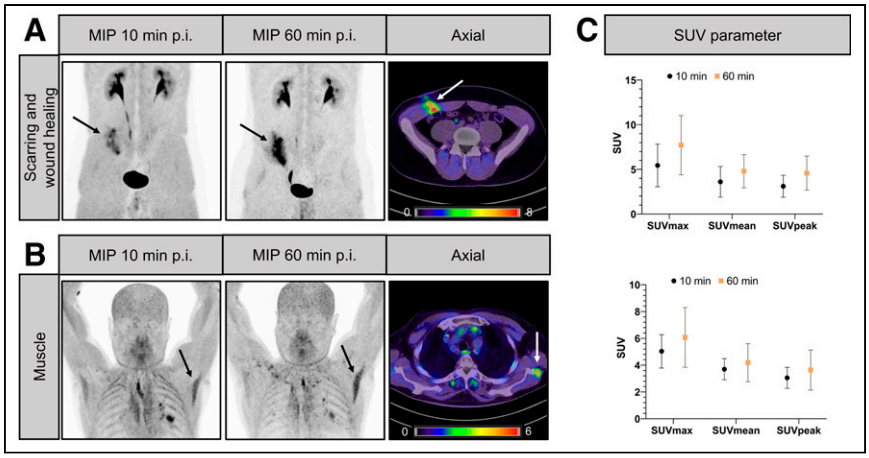

FIGURE 3. Scarring, wound healing, and muscle uptake. (A) Focal uptake along access route after surgical or interventional procedures can be observed, such as after tumor resection of round cell sarcoma of right abdominal wall. (B) Localized, isolated increased uptake is observed in larger muscles and tendon insertions. (C) Both findings show stable uptake values over 60 min. MIP = maximum-intensity projection; p.i. = after injection.

therefore categorized as unspecific. Comparison of distributions showed no statistically significant differences in findings between ^{68}Ga-FAPI-04 and ^{68}Ga-FAPI-46 (Table 2). A detailed description of uptake locations for degenerative, muscle, and scar/wound healing is given in Supplemental Table 1 (supplemental materials are available at http://jnm.snmjournals.org). Uptake values for the categories are shown in Table 3, and ^{68}Ga-FAPI-04 and ^{68}Ga-FAPI-46 uptake for the respective categories is additionally discriminated in Supplemental Table 2. Here, we will discuss the findings and pitfalls by category.

Degenerative Pitfalls

Common pitfall findings were degenerative lesions, mostly associated with joints and vertebral bones (51.6%), with no significant difference between ^{68}Ga-FAPI-04 and ^{68}Ga-FAPI-46 ($P = 0.41$) (Table 2). The lesions showed focal uptake with a mean SUV_{max} of 7.7 ± 2.9 (Table 3). Figure 2 depicts a case of uptake in the facet joints of the lumbar vertebrae with degenerative features on CT (Fig. 2A), as well as a case of focal uptake in the left temporomandibular joint (Fig. 2B). SUV parameters showed a significant increase in SUV_{max} (mean SUV_{max}, 6.3 ± 2.5 vs. 7.7 ± 2.9, $P = 0.04$) but no difference between early and late imaging timepoints for SUV_{mean} and SUV_{peak} (mean SUV_{peak}, 3.8 ± 1.6 vs. 4.3 ± 1.8, $P = 0.19$; mean SUV_{mean}, 3.7 ± 1.7 vs. 4.3 ± 1.8, $P = 0.14$) (Fig. 2C).

Scarring/Wound Healing and Muscle Uptake

Focal or localized muscle uptake was observed in 28.6%, with a mean SUV_{max} of 6.1 ± 2.2, and uptake in scars or wound-healing processes was found in 19.8%, with a mean SUV_{max} of 7.7 ± 3.3 (Tables 2 and 3). Sites with a predilection for muscle uptake were larger muscle groups such as the quadriceps femoris muscle, latissimus dorsi muscle, triceps muscle, and autochthone muscles. SUV parameters did not differ between early and late imaging either in muscle uptake findings (mean SUV_{max}, 5.0 ± 1.3 vs. 6.1 ± 2.2, $P = 0.06$) or in scarring and wound-healing processes (mean SUV_{max}, 5.4 ± 2.4 vs. 7.7 ± 3.3, $P = 0.08$) (Fig. 3).

Head-and-Neck Pitfalls

In 41 patients (45.1%), uptake could be found in the head and neck, most frequently localized in the extraocular muscles, the salivary glands, the oral or nasal mucosa, or focally in the teeth (Fig. 4, top panel). The salivary glands showed a significant decrease in uptake from early to late imaging timepoints (SUV_{max}, 6.0 ± 1.2 vs. 3.2 ± 0.2; SUV_{mean}, 4.4 ± 0.8 vs. 2.4 ± 0.2; SUV_{peak}, 3.7 ± 0.7 vs. 2.1 ± 0.3 [$P < 0.05$]). Uptake in the extraocular muscle and teeth was stable between 10 and 60 min after injection (Fig. 4, middle and bottom panels).

Uterine and Mammary Findings

Intense, variable uptake in the uterus occurred in 66.7% of all female patients ($n = 36$; posthysterectomy patients excluded) (SUV_{max} 60 min after injection, 12.2 ± 7.3; range, 4.2–31.2). Younger women, in particular, showed higher uptake in the uterus, with a negative correlation between SUV parameters and age (SUV_{max}, $r = -0.6$, $P < 0.01$; SUV_{peak}, $r = -0.57$, $P < 0.01$;

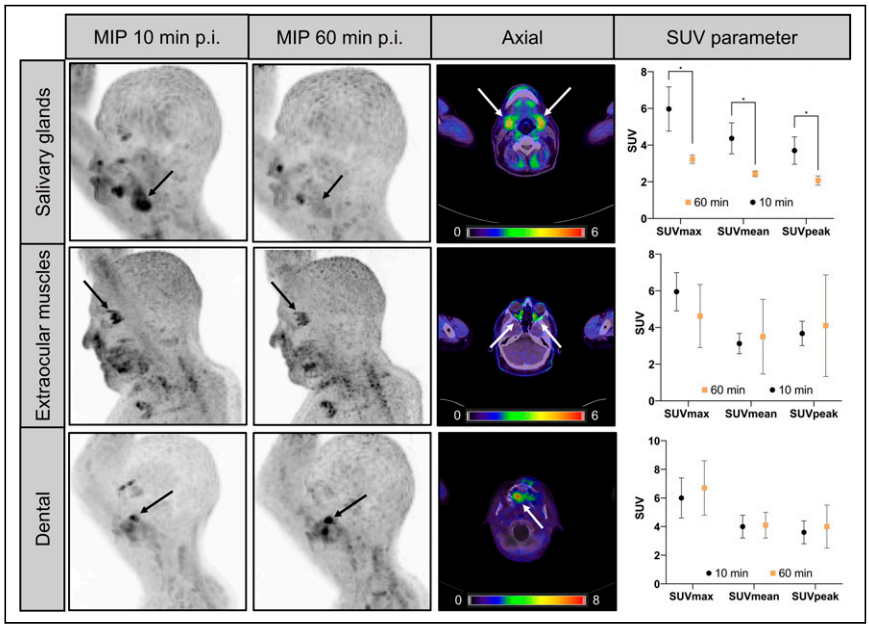

FIGURE 4. Head-and-neck findings. Salivary glands show significant decrease in uptake from 10 to 60 min after injection ($P < 0.05$). Few patients have increased uptake in extraocular muscles. Dental foci are often reported most likely linked to chronic inflammatory processes. MIP = maximum-intensity projection; p.i. = after injection

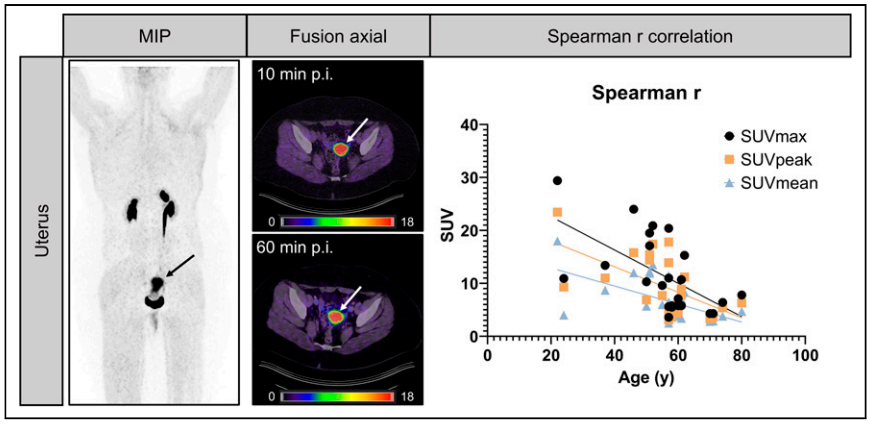

FIGURE 5. Uterine findings. Of female patients (posthysterectomy patients excluded), 66.7% showed fibroblast activation of uterus. Uterine uptake has moderate to strong negative correlation with age (SUV_{max}, $r = -0.6$, $P < 0.01$; SUV_{peak}, $r = -0.57$, $P < 0.01$; SUV_{mean}, $r = -0.58$, $P < 0.01$), possibly linked to menopausal shrinkage. MIP = maximum-intensity projection; p.i. = after injection.

SUV_{mean}, $r = -0.58$, $P < 0.01$) (Fig. 5). As depicted in Figure 6, few patients (7.7%) showed increased uptake in the mammary glands; uptake was stable over 60 min, with a mean SUV_{max} of 4.5 ± 1.5 at 60 min after injection. Age ranged from 24 to 67 y in these female patients.

DISCUSSION

FAP-directed ^{68}Ga-FAPI PET/CT is a novel modality introduced for imaging of various entities. Recent studies have demonstrated comparable or even increased detection rates in comparison with ^{18}F-FDG PET/CT, such as in pancreatic cancer, sarcoma, and hepatic malignancies (*9,10,20*). In the interpretation of ^{68}Ga-FAPI PET/CT scans, the readers—especially at centers to which this technology was recently introduced—need to be informed about common findings and potential pitfalls. This pictorial analysis aimed to summarize ^{68}Ga-FAPI PET/CT uptake patterns and common interpretation pitfalls that were recorded in our retrospective database.

Further, we aimed to report uptake intensity, location, and frequency of occurrence. In our opinion, such a report is of great importance in avoiding misdiagnosis, as this novel modality will soon become more widespread.

We found that unspecific or nontarget uptake can be observed in degenerative, traumatic, inflammatory, and physiologic processes, and we were able to show that non–tumor-specific or unspecific uptake is present in most patients at a variety of locations, but especially in degenerative spine conditions. In our cohort, uterine uptake was noted in 66.7% of women and showed a decrease in intensity with age. Hypothetically, this is due to the decreased FAP expression of the endometrium after menopause, as is supported by proteomic data and PET data on the FAP expression of the endometrium before and after menopause (*16,21,22*). This decreased expression might pose an important pitfall and limitation in the use of ^{68}Ga-FAPI PET/CT for local staging of gynecologic cancers and should be take into consideration, but larger cohorts are needed to verify this finding.

Furthermore, we observed in nearly half of patients non–tumor-related uptake in the head-and-neck region. Interestingly, the salivary glands showed a decrease in tracer retention within the first hour after injection, but a thorough literature review did not reveal the underlying mechanism. This observation might reflect unspecific tracer accumulation, which should be considered when patients with head-and-neck cancer are being imaged; these tumors might benefit from use of later imaging timepoints. Additionally, intense uptake in the extraocular muscles was noted in 9% of the patients; however, these patients had no medical history of major ocular disorders and, to date, no specific data on FAP expression in these muscles is available.

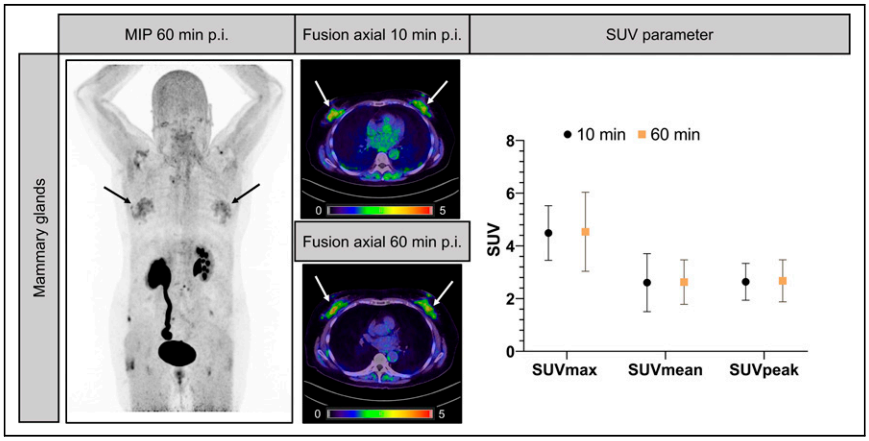

FIGURE 6. Mammary gland findings. Rarely, patients showed increased uptake in mammary tissue (7.7%). Uptake was reported in middle-aged women and one man with gynecomastopathy. Additionally, other non–tumor-specific uptake around shoulder and hip joints can be seen, as well as tracer accumulation in urinary tract. MIP = maximum-intensity projection; p.i. = after injection.

Previous studies demonstrated decreasing uptake in pancreatitis and other, unspecified, inflammatory diseases (*9,17,23*). In contrast, in our study dental foci of active inflammation showed increased uptake over time, possibly due to unspecific uptake in surrounding edema.

Numerous studies provide data on FAP overexpression in carcinoma-associated fibroblasts and in various other processes, such as fibrosis, inflammatory atheromata, and osteoarthritis (*24–27*). FAP is overexpressed by myofibroblasts in tissue remodeling, wound healing, and fibrotic tissue (*28*). This phenomenon has already been found by our group and others that studied patients after myocardial infarction using ^{68}Ga-FAPI PET/CT (*29–31*). In those patients, ^{68}Ga-FAPI uptake matched

the affected myocardium, most likely due to ongoing remodeling processes, and agrees with scientific evidence on fibroblast activation after ischemia (*32,33*).

Pitfalls may originate from specific uptake through an increased FAP expression level and mechanisms of unspecific uptake, including edema, tracer extravasation, and some inflammatory disorders. Future studies should aim to thoroughly validate positive ^{68}Ga-FAPI PET/CT findings via immunohistochemical FAP expression (*10,34*).

Our study comes with several limitations. Our single-center analysis consisted of a heterogeneous cohort with various oncologic and nononcologic diseases and at different disease stages. In addition, we analyzed 2 different FAPI tracers, which might have different frequencies of certain pitfalls, although such differences were not observed in our cohort. Lastly, the list of common findings we have reported here is not intended to be exhaustive and cannot give proper answers about the underlying pathophysiologic processes. Future studies should elucidate disease- and tracer-specific pitfalls and common findings. Because the implementation of ^{68}Ga-FAPI PET is expanding, it is important to share pitfalls and common findings now, especially for centers that have recently introduced this new technology.

CONCLUSION

Here, we have reported non–tumor-specific ^{68}Ga-FAPI uptake—especially in degenerative lesions, wound healing, muscles, and the uterus—as a potential pitfall in the interpretation of ^{68}Ga-FAPI PET/CT images. This report will help readers improve the accuracy of image interpretation at centers that have recently begun using ^{68}Ga-FAPI PET/CT. Our work can be seen as an initial guide to the reporting of ^{68}Ga-FAPI PET/CT, a novel and rapidly expanding imaging modality.

DISCLOSURE

Wolfgang Fendler reports fees from BTG (consultant), Calyx (consultant), RadioMedix (image reader), Bayer (speakers bureau), and Parexel (image reader) outside the submitted work. Rainer Hamacher is supported by the Clinician Scientist Program of the University Medicine Essen Clinician Scientist Academy (UMEA), sponsored by the faculty of medicine and Deutsche Forschungsgemeinschaft (DFG), and has received travel grants from Lilly, Novartis, and PharmaMar, as well as fees from Lilly outside the submitted work. Lukas Kessler is a consultant for BTG and AAA and received fess from Sanofi outside the submitted work. Justin Ferdinandus has received a Junior Clinician Scientist Stipend granted by the University Duisburg–Essen. Manuel Weber is a consultant for Boston Scientific and received fees outside the submitted work. Christoph Rischpler reports grants and other fees from Pfizer; other fees from Alnylam, GE, Siemens, and Advanced Accelerator Applications; and personal fees from Pharmtrace outside the submitted work. Katharina Lueckerath reports paid consulting activities for Sofie Biosciences/iTheranostics and funding from AMGEN outside the submitted work. No other potential conflict of interest relevant to this article was reported.

KEY POINTS

QUESTION: Is there an association between ^{68}Ga-FAPI uptake intensity and FAP expression in bone and soft-tissue sarcomas, and what is the diagnostic performance of ^{68}Ga-FAPI PET in sarcoma patients?

PERTINENT FINDINGS: We observed an association between ^{68}Ga-FAPI uptake intensity and immunohistochemical FAP expression in sarcomas and showed ^{68}Ga-FAPI PET to have high accuracy in sarcoma patients.

IMPLICATIONS FOR PATIENT CARE: ^{68}Ga-FAPI PET has diagnostic utility for patients with sarcoma and future implications in FAP-targeted therapies.

REFERENCES

1. Koczorowska MMM, Tholen S, Bucher F, et al. Fibroblast activation protein-α, a stromal cell surface protease, shapes key features of cancer associated fibroblasts through proteome and degradome alterations. *Mol Oncol.* 2016;10:40–58.
2. Kalluri R. The biology and function of fibroblasts in cancer. *Nat Rev Cancer.* 2016;16:582–598.
3. Rettig WJ, Garin-Chesa P, Beresford HR, Oettgen HF, Melamed MR, Old LJ. Cell-surface glycoproteins of human sarcomas: differential expression in normal and malignant tissues and cultured cells. *Proc Natl Acad Sci USA.* 1988;85:3110–3114.
4. Niedermeyer J, Garin-Chesa P, Kriz M, et al. Expression of the fibroblast activation protein during mouse embryo development. *Int J Dev Biol.* 2001;45:445–447.
5. Liu F, Qi L, Liu B, et al. Fibroblast activation protein overexpression and clinical implications in solid tumors: a meta-analysis. *PLoS One.* 2015;10:e0116683.
6. Loktev A, Lindner T, Burger E-M, et al. Development of fibroblast activation protein–targeted radiotracers with improved tumor retention. *J Nucl Med.* 2019;60:1421–1429.
7. Giesel FL, Kratochwil C, Lindner T, et al. ^{68}Ga-FAPI PET/CT: biodistribution and preliminary dosimetry estimate of 2 DOTA-containing FAP-targeting agents in patients with various cancers. *J Nucl Med.* 2019;60:386–392.
8. Kratochwil C, Flechsig P, Lindner T, et al. ^{68}Ga-FAPI PET/CT: tracer uptake in 28 different kinds of cancer. *J Nucl Med.* 2019;60:801–805.
9. Röhrich M, Naumann P, Giesel FL, et al. Impact of ^{68}Ga-FAPI PET/CT imaging on the therapeutic management of primary and recurrent pancreatic ductal adenocarcinomas. *J Nucl Med.* 2021;62:779–786.
10. Kessler L, Ferdinandus J, Hirmas N, et al. ^{68}Ga-FAPI as a diagnostic tool in sarcoma: data from the ^{68}Ga-FAPI PET prospective observational trial. *J Nucl Med.* 2022;63:89–95.
11. Lin R, Lin Z, Zhang J, Yao S, Miao W. Increased ^{68}Ga-FAPI-04 uptake in Schmorl node in a patient with gastric cancer. *Clin Nucl Med.* 2021;46:700–702.
12. Can C, Gündoğan C, Güzel Y, Kaplan İ, Kömek H. ^{68}Ga-FAPI uptake of thyroiditis in a patient with breast cancer. *Clin Nucl Med.* 2021;46:683–685.
13. Liu H, Chen Z, Yang X, Fu W, Chen Y. Increased ^{68}Ga-FAPI uptake in chronic cholecystitis and degenerative osteophyte. *Clin Nucl Med.* 2021;46:601–602.
14. Gündoğan C, Güzel Y, Can C, Alabalik U, Kömek H. False-positive ^{68}Ga-fibroblast activation protein-specific inhibitor uptake of benign lymphoid tissue in a patient with breast cancer. *Clin Nucl Med.* 2021;46:e433–e435.
15. Wu J, Liu H, Ou L, Jiang G, Zhang C. FAPI uptake in a vertebral body fracture in a patient with lung cancer. *Clin Nucl Med.* 2021;46:520–522.
16. Dendl K, Koerber SA, Adeberg S, et al. Physiological FAP-activation in a postpartum woman observed in oncological FAPI-PET/CT. *Eur J Nucl Med Mol Imaging.* 2021;48:2059–2061.
17. Ferdinandus J, Kessler L, Hirmas N, et al. Equivalent tumor detection for early and late FAPI-46 PET acquisition. *Eur J Nucl Med Mol Imaging.* 2021;48:3221–3227.
18. Rischpler C, Beck TI, Okamoto S, et al. ^{68}Ga-PSMA-HBED-CC uptake in cervical, celiac, and sacral ganglia as an important pitfall in prostate cancer PET imaging. *J Nucl Med.* 2018;59:1406–1411.
19. Sheikhbahaei S, Afshar-Oromieh A, Eiber M, et al. Pearls and pitfalls in clinical interpretation of prostate-specific membrane antigen (PSMA)-targeted PET imaging. *Eur J Nucl Med Mol Imaging.* 2017;44:2117–2136.

20. Shi X, Xing H, Yang X, et al. Fibroblast imaging of hepatic carcinoma with ^{68}Ga-FAPI-04 PET/CT: a pilot study in patients with suspected hepatic nodules. *Eur J Nucl Med Mol Imaging.* 2021;48:196–203.
21. Uhlén M, Fagerberg L, Hallstrom BM, et al. Tissue-based map of the human proteome. *Science.* 2015;347:1260419-1260419.
22. Dendl K, Koerber SA, Finck R, et al. ^{68}Ga-FAPI-PET/CT in patients with various gynecological malignancies. *Eur J Nucl Med Mol Imaging.* 2021;48:4089–4100.
23. Schmidkonz C, Rauber S, Atzinger A, et al. Disentangling inflammatory from fibrotic disease activity by fibroblast activation protein imaging. *Ann Rheum Dis.* 2020;79:1485–1491.
24. Wang XM. Fibroblast activation protein and chronic liver disease. *Front Biosci.* 2008;13:3168–3180.
25. Milner JM, Kevorkian L, Young DA, et al. Fibroblast activation protein alpha is expressed by chondrocytes following a pro-inflammatory stimulus and is elevated in osteoarthritis. *Arthritis Res Ther.* 2006;8:R23.
26. Brokopp CE, Schoenauer R, Richards P, et al. Fibroblast activation protein is induced by inflammation and degrades type I collagen in thin-cap fibroatheromata. *Eur Heart J.* 2011;32:2713–2722.
27. Kelly T, Huang Y, Simms AE, Mazur A. Fibroblast activation protein-α. In: *International Review of Cell and Molecular Biology*. Elsevier; 2012:83–116.
28. Scharl M, Huber N, Lang S, Fürst A, Jehle E, Rogler G. Hallmarks of epithelial to mesenchymal transition are detectable in Crohn's disease associated intestinal fibrosis. *Clin Transl Med.* 2015;4:1–9.
29. Kessler L, Kupusovic J, Ferdinandus J, et al. Visualization of fibroblast activation after myocardial infarction using ^{68}Ga-FAPI PET. *Clin Nucl Med.* 2021;46:807–813.
30. Diekmann J, Koenig T, Zwadlo C, et al. Molecular imaging identifies fibroblast activation beyond the infarct region after acute myocardial infarction. *J Am Coll Cardiol.* 2021;77:1835–1837.
31. Zhu W, Guo F, Wang Y, Ding H, Huo L. ^{68}Ga-FAPI-04 accumulation in myocardial infarction in a patient with neuroendocrine carcinoma. *Clin Nucl Med.* 2020; 45:1020–1022.
32. Varasteh Z, Mohanta S, Robu S, et al. Molecular imaging of fibroblast activity after myocardial infarction using a ^{68}Ga-labeled fibroblast activation protein inhibitor, FAPI-04. *J Nucl Med.* 2019;60:1743–1749.
33. Tillmanns J, Hoffmann D, Habbaba Y, et al. Fibroblast activation protein alpha expression identifies activated fibroblasts after myocardial infarction. *J Mol Cell Cardiol.* 2015;87:194–203.
34. Shi X, Xing H, Yang X, et al. Comparison of PET imaging of activated fibroblasts and ^{18}F-FDG for diagnosis of primary hepatic tumours: a prospective pilot study. *Eur J Nucl Med Mol Imaging.* 2021;48:1593–1603.